UCRL-91738
PREPRINT

Photothermal Lensing Measurements of Two-Photon Absorption and Two-Photon-Induced Color Centers in Borosilicate Glasses at 532 nm

W. T. White, III
M. A. Henesian
M. J. Weber

This paper was prepared for submittal to
J. Opt. Soc. Am. (B)

October 28, 1984

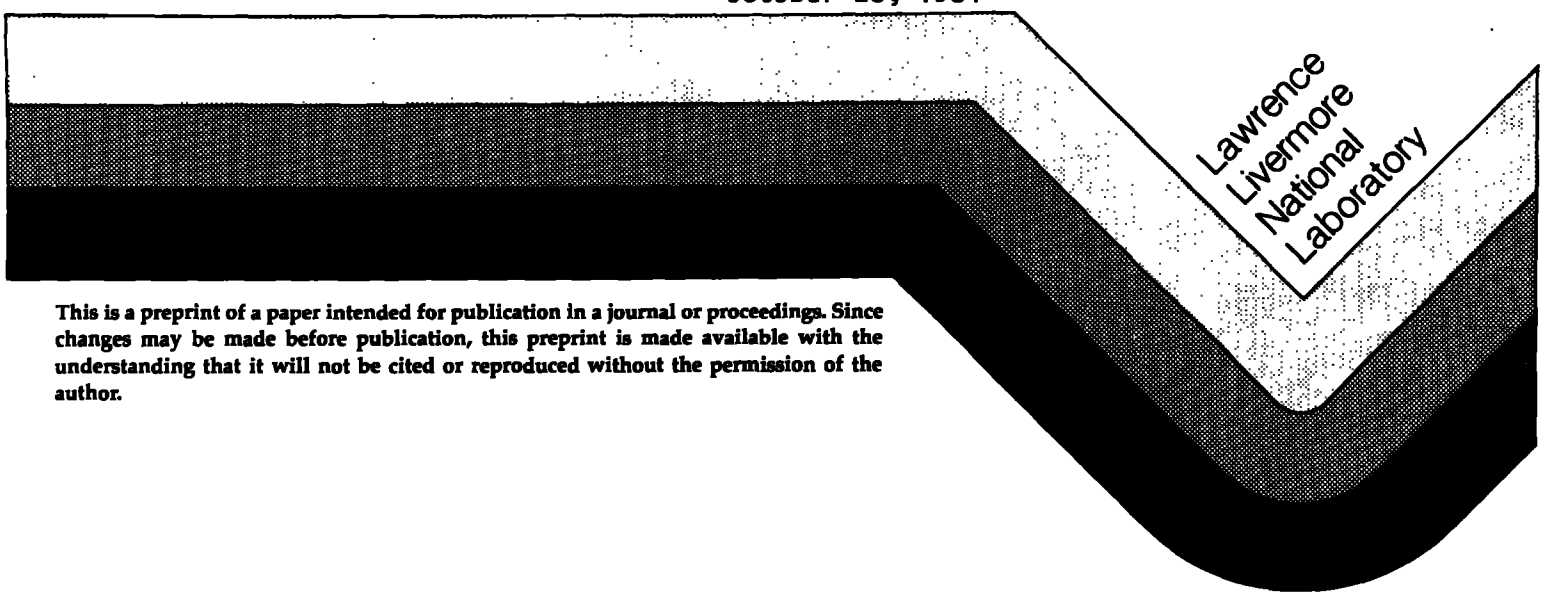

Photothermal Lensing Measurements of Two-Photon Absorption and Two-Photon-Induced Color Centers in Borosilicate Glasses at 532 nm*

W. T. White III, M. A. Henesian, and M. J. Weber

Lawrence Livermore National Laboratory

University of California

Livermore, California 94550

ABSTRACT

Using photothermal lensing we have measured two-photon absorption coefficients and have observed laser-induced solarization at 532 nm in the transparent borosilicate glasses BK-3, BK-7, and BK-10. The two-photon absorption coefficients at 532 nm are 0.6, 2.9, and 0.4 cm/TW for BK-3, BK-7, and BK-10, respectively. This is approximately two orders of magnitude smaller than the two-photon absorption coefficients of crystalline materials of comparable energy band gap. Our results in BK-7 indicate that a two-photon process initiates the solarization and that one-photon bleaching limits it. The maximum induced absorption at 532 nm in BK-7 is approximately 0.07 cm^{-1} per GW/cm^2.

*Work performed under the auspices of the Division of Materials Sciences, Office of Basic Energy Sciences, U.S. Department of Energy by the Lawrence Livermore National Laboratory under Contract No. W-7405-ENG-48.

Photothermal Lensing Measurements of Two-Photon Absorption and Two-Photon-Induced Color Centers in Borosilicate Glasses at 532 nm

W. T. White III, M. A. Henesian, and M. J. Weber

Lawrence Livermore National Laboratory

University of California

Livermore, California 94550

Introduction

Using photothermal lensing we have measured two-photon absorption (2PA) coefficients[1] and have observed laser-induced discoloration ("solarization") at 532 nm in the borosilicate optical glasses BK-3, BK-7, and BK-10. These materials are used commonly in optical components for visible lasers. Although at low intensities these glasses are highly transparent, they absorb measurably and discolor under intense (GW/cm^2) visible and ultraviolet laser irradiation.[2] Such optical losses are important to consider in the design of high-intensity, high-repetition-rate laser systems.

The measurements reported in this paper are the first made in borosilicate glasses at 532 nm and are the first photothermal lensing measurements of nonlinear absorption in any transparent glass. Previously, Hagen and Snitzer reported on the laser-induced solarization in flint glass at 532 nm.[3]. Nonlinear absorption measurements in borosilicate glasses were made at 351 nm by Smith, who used a direct transmittance technique[2]. Both in Smith's work and in the results reported here, the measured 2PA coefficients of glass are typically one hundred times smaller than 2PA coefficients of crystals of comparable energy band gaps.[4]

Photothermal Lensing

Photothermal lensing belongs to a class of optical techniques for detecting small temperature changes in a sample due to absorption of a beam of light. Related techniques include photothermal displacement,[5] photothermal deflection,[6] photoacoustic detection,[7] thermal calorimetry,[8] and photothermal interferometry.[9] Of these techniques, photothermal lensing, photothermal deflection, and photothermal interferometry probe bulk materials while completely avoiding spurious signals due to absorption of scattered light by a transducer affixed to the sample. The high sensitivity of photothermal lensing and photothermal deflection make these methods suitable for measuring weak absorptions such as 2PA in transparent optical materials.[10] The choice of one method over the other is a matter of preference, since their sensitivities are comparable.[6] Twarowski and Kliger have successfully measured 2PA in certain organic liquids using photothermal lensing.[1] We have used the same method in our measurements of 2PA in glasses.

In photothermal lensing the absorption of a beam of light changes the local temperature distribution inside a sample. As a result, the refractive index n of the sample, through its temperature dependence, exhibits a spatial variation, forming a "thermal lens." A second beam of light, the "probe beam," monitors the thermal lens caused by the first beam of light, the "pump beam." The pump and probe beams may in practice be the same beam, although this is not necessary.[11] When the probe beam is centered on the thermal lens, the principal effect of the lens is

to change the divergence of the probe, which alters the far-field axial intensity of the probe. The fractional change in the far field axial intensity is then measured.

To generate sufficient intensity with sub-band-gap photons for observable 2PA in transparent optical glasses, one must use Q-switched laser pulses. For m-photon absorption of a Q-switched pump beam with a Gaussian spatial profile, the time-dependent focusing power of the thermal lens is given by 1/f, where in the thin, wide lens approximation[1]

$$1/f = \frac{1/f_o}{(1 + 2mt/t_c)^2} \quad . \tag{1}$$

In Eq. (1) the Q-switched pulse arrives at time t=0. The peak focusing power ($1/f_o$) and the thermal diffusion time (t_c) are given by the following expressions:

$$1/f_o = \frac{4m\,(1-\eta)\,\Gamma^m\,H^{(m)}\beta^{(m)}}{w_p^2\;C} \quad \frac{\partial(n\ell-\ell)}{\partial T} \tag{2}$$

and

$$t_c = w_p^2/4D \quad . \tag{3}$$

Here w_p is the Gaussian $1/e^2$ radius of the pump beam intensity at the sample (cm), D is the thermal diffusivity (cm^2/s), C is the specific heat per unit volume of the sample ($J/cm^3/K$), η is the effective luminescent efficiency of the sample, and $\partial(n\ell-\ell)/\partial T$ is the temperature derivative of the optical path length (K^{-1}). Γ is the axial fluence of the pump beam inside the sample (J/cm^2), $\beta^{(m)}$ is the m-photon absorption coefficient of the sample (cm^{-1} per $(W/cm^2)^{m-1}$),

ℓ is the sample thickness (cm), and $H^{(m)}$ is the m-th moment of normalized axial pump beam intensity (s^{1-m}) defined as

$$H^{(m)} = \int_0^\infty (I_p(t)/I)^m dt. \tag{4}$$

In many thermal lensing experiments, including ours, the pump laser fires repetitively at a fixed interval of time, Δt. For a sufficiently large number of shots a thermal background builds up, and one may separate Eq. (1) into two terms, the contribution from the most recent pulse and the background due to all previous pulses. For rapid thermal diffusion ($t_c << \Delta t$), the background contribution to 1/f is negligible, even in the limit of many pulses.

For a continuous-wave Gaussian probe beam, the axial intensity a distance z past the thin thermal lens is

$$I_2\,(1/f) = \frac{I_1}{(1 + \frac{z}{R_1} - \frac{z}{f})^2 + (\frac{z\lambda}{\pi w_1^2})^2}\,, \tag{5}$$

where I_1 and I_2 refer to the probe axial intensity at the sample and in the plane of observation, respectively, w_1 denotes the size of the probe beam $1/e^2$ Gaussian radius at the sample, λ is the optical wavelength of the probe outside the sample, and $1/R_1$ is the curvature of the phase front of the probe beam incident at the sample. The sign conventions are chosen so that $R_1>0$ implies a diverging wave while $f>0$ implies a focusing ("positive") lens.

The thermal lensing signal S is defined as the fractional change in probe beam axial intensity relative to I_2 in the absence of a thermal

lens. For an optical detector whose output is proportional to intensity, S is given by the following approximation, which includes only terms linear in 1/f:

$$S = \frac{2\pi}{\lambda} \frac{\partial(n\ell-\ell)}{\partial T} \frac{\beta^{(m)} I^m H^{(m)} (1-\eta)}{C} G(t) \quad , \tag{6}$$

where G is a beam-geometry-dependent thermal dissipation factor. One can show that in the model of Twarowski[1] and others

$$G(t) = \frac{B\ 4m\ w_1^2/w_p^2}{(1+B^2)(1+2mt/t_c)^2} \quad , \tag{7}$$

where

$$B = \frac{\pi w_1^2}{\lambda} (1/R_1 + 1/z) \quad . \tag{8}$$

Such a model implicitly assumes that the thermal lens is much wider than the probe beam. When the thermal lens is not much wider than the probe beam, as was the case in our experiment, spherical aberrations affect the axial intensity I_2 so that in general for a Gaussian probe and a thin Gaussian-shaped lens

$$G(t) = \frac{B\ 4m\ w_1^2/w_p^2}{(1+2mw_1^2/w_p^2+2mt/t_c)^2 + B^2(1+2mt/t_c)^2} \quad . \tag{9}$$

Equation (9) is identical to Equation (7) when $1 >> 2mw_1^2/w_p^2$. It is obtained by solving the Fresnel propagation integral in the weak lensing regime for the axial intensity due to a Gaussian TEM_{oo} wave impinging upon a thin Gaussian-shaped lens and propagating a distance z.[12]

Experimental Apparatus and Techniques

Figure 1 illustrates our experimental arrangement. A nominally 5-ns pump was derived from a frequency-doubled, Q-switched Nd:YAG laser (Molectron MY-34) operating at 10 Hz. Spatially smooth, high-intensity illumination was obtained at the sample by focusing the apertured beam to a waist about 10 cm past the sample. A power stabilized helium-neon probe laser (Spectra Physics 124 B) was focused by lens L2 (f=1.0 m) to a position 10-20 cm past the sample (W_o in Fig. 1). The pump and probe beams were carefully overlapped in the sample to ensure that photothermal deflection[6] did not contribute to the lensing signal. After the two beams were spatially separated by dichroic mirror BS3, the remaining stray light along the probe beam path was blocked by narrow bandpass filter F1. In the absence of a sample, there was no signal due to pump beam leakage or spurious thermal lensing. Aperture A3, which was approximately 1.8 m from the sample, transmitted a 1-mm diameter axial section of the 12-mm diameter probe beam to a large area silicon photodiode (United Detector Technology PIN8LC). The amplified detector output was averaged (PAR 4203 signal averager and PAR 162 gated integrator). The peak voltage change and the DC voltage corresponding to the "unlensed" probe beam were then recorded for subsequent analysis.

To quantify 2PA coefficients, accurate characterization of the temporal and spatial pump beam profile was essential. These profiles are shown in Figs. 2 and 3. The central spike of the tri-lobed temporal pulse contained approximately 70% of the pulse energy and fluctuated about $\pm$12% in amplitude on a shot-to-shot basis. The spatial beam profile was smooth with a half-maximum diameter of approximately 0.2 mm. The

probe beam was slightly larger, about 0.3-mm FWHM. Figures 2 and 3 are the result of averaging 32 consecutive pulses. Temporal characterization of the pump beam was achieved with a fast silicon photodiode and a transient digitizer (Tektronix R7912). Spatial characterization of the pump beam was obtained with a video image analysis system (Grinnell GMR-27-10) synchronized with a microcomputer (LSI 11/23) at the 10 Hz laser rate. Pump beam energy was monitored with a volumetric absorbing calorimeter (Scientech 361).

As calibration standards we used two neodymium-doped BK-7 glass samples (0.16 and 0.8 weight-percent Nd_2O_3) prepared in thicknesses of 1, 2, and 10 mm each. When normalized by doping concentration, thickness, and fluence, every reference sample yielded the same thermal lensing signal to within ± 2%. Thus, surface effects in the reference samples were negligible when compared to bulk effects, and the thin lens assumption was valid even for samples in excess of 10 mm thickness. The peak thermal lensing signal varied linearly with pump beam fluence for modulation in the probe beam axial intensity of up to 40%. This established the linear regime of the thermal lensing signal in our experiment.

Heating in the calibration samples from nonradiative Nd^{3+} transitions following absorption of 532 nm light was calculated from the estimated quantum efficiency for 0.16 and 0.8 weight-percent Nd_2O_3 samples and from radiative branching ratios of the $^4F_{3/2} \rightarrow {}^4I_J$, (J=15/2, 13/2, 11/2, 9/2) transitions of Nd^{3+} in the BK-7 host.[13] All other Nd transitions were treated as quasi-instantaneous, non-radiative processes. A radiative efficiency of 0.74 for the

$^4F_{3/2}$ level and branching ratios of 0.004, 0.092, 0.485, and 0.419 gave an overall effective radiation efficiency of $\eta = 0.42$ in the doped calibration samples following 532 nm excitation. Non-radiative decay by ion-ion cross relaxation was not a strong effect at the Nd concentrations used.

We measured the thermal lensing in undoped BK-3, BK-7, and BK-10 in two steps. First, we measured the relative 2PA coefficients among the three glasses, carefully limiting the number of pulses irradiating a given site in order to avoid solarization. Then we measured the solarization by exposing a single site to a 10 Hz stream of pulses at a fixed fluence for times as long as 2 hours. Normalizing the peak signals by fluence squared, by sample thickness, and by the thermal parameter $(\partial(n\ell-\ell)/\partial T)/\ell C$ yielded the relative 2PA coefficients from Eq. (6). Table 1 shows the values of $(\partial(n\ell-\ell)/\partial T)/\ell$ and C for each of the glasses. The quantity η was assumed to be zero in the undoped glasses, and the geometric beam-size paramter G(0) was independent of the thermal lensing medium, apart from the parameter m. (For 1PA, m=1; for 2PA, m=2.) We obtained our undoped samples from Schott Glass Technologies Inc. and our Nd-doped reference samples from the National Bureau of Standards.

Signal distortions due to strong thermal lensing were believed insignificant, since we operated only within our experimentally determined linear photothermal lensing regime. Also, signal distortions due to self-focusing were discounted on the basis of measured and calculated values of n_2 in the samples.[14]

Detectivity in our experiment was limited by 0.3% rms power supply ripple at audio frequencies in the probe laser and by laser damage to the samples. To improve the signal-to-noise ratio, we filtered the probe beam signal with a DC-10 kHz bandpass filter. The power supply noise could not be completely suppressed, because it was nearly synchronous with the 10 Hz laser pulse rate. We estimate the lower limit of detectable absorption to be $\alpha_{eff}\ell\Gamma = 2$ mJ/cm^2, for long-term averaging (1000 shots) of the probe beam signal at a signal-to-noise ratio of 2:1. For a sample thickness of $\ell = 1$ cm and pump beam axial fluence of $\Gamma = 20$ J/cm^2, this corresponds to $\alpha_{eff} = 10^{-4}$ cm^{-1}.

Results

Table 2 shows the measured 2PA coefficients and the band edge energies for BK-3, BK-7, and BK-10. The 2PA coefficients were determined from the slope of a fit of thermal lensing signal vs fluence squared. Linear absorption at 532 nm as measured with a Cary 17 spectrophotometer was less than 0.3% cm^{-1} in all three glasses. As shown in Table 2, 2PA is energetically allowed in all samples, but intrinsic 1PA is energetically forbidden. The observed quadratic dependence of signal upon fluence indicates a two-photon absorption process, either instantaneous or step-wise.

Although 2PA is energetically allowed for all three borosilicate glasses tested, the energy of two 532 nm photons only slightly exceeds the band edge energies of BK-3 and BK-10. Since the density of electron states is much lower on the toe of the absorption curve than on the knee, one expects 2PA at 532 nm to be weaker in BK-3 and BK-10 than in BK-7. Table 2 shows that this is so. Because the absorption is much weaker in

BK-3 and BK-10, the signal-to-noise ratio is lower, as is evident from Table 2. For comparison, we attempted to measure 2PA in fused silica (7.3 eV band edge)[4] but found none within the limits of accuracy of our measurement. This agrees with work by Smith at 351 nm.[2]

Among the three glasses tested, BK-7 solarizes most readily under given conditions of illumination. A smoky brown discoloration occurs after many shots (10-2000, depending upon intensity) and is visible to the unaided eye. The solarization is thermally stable at room temperature. In contrast, the 532-nm laser-induced solarization in BK-3 and in BK-10 is too weak to see with the eye, even through a loupe. The rise in absorption in BK-3 and in BK-10 is barely detectable with thermal lensing, even after exposure to 20,000 laser pulses at intensities near optical damage threshold.

Figure 4 shows the 2PA-induced linear absorbance spectrum of a heavily solarized BK-7 sample. The induced absorption has a long tail extending across the visible and into the infrared past 1.0 μm. It exhibits a small, broad feature in the vicinity of the pump wavelength at 532 nm, and then it rises rapidly at wavelengths below 400 nm. The absorbance was measured with a Cary 17 spectrophotometer after a 2.5-mm diameter raster pattern of closely spaced spots had been generated in a 1-cm thick sample. Each spot was irradiated over six thousand times at a laser fluence of about 20 J/cm^2. The limited dynamic range of the spectrophotometer prevented the resolution of the spectral structure below about 320 nm in the solarized BK-7.

Figure 5 graphs induced absorption of BK-7 versus thousands of laser shots at three fluences. As shown in the figure, the absorption first rises and then reaches a fluence-dependent steady-state value with

repeated exposure, indicating the existence of a saturation mechanism. The most likely mechanisms which could account for saturation in an experiment such as ours are thermal relaxation and photobleaching.

For two reasons, thermal relaxation is believed to be an insignificant limitation of solarization in our experiments. First, at room temperature the solarization in BK-7 does not spontaneously diminish. This has been demonstrated in several samples which were solarized over two years ago by us and which still remain visibly discolored. Second, although the samples can be thermally annealed, temperatures in excess of 400K are required. The laser-induced temperature rises in our samples are easily estimated to be less than 1K, too small to have an important effect. Therefore neither spontaneous nor induced thermal relaxation is expected to contribute significantly to the saturation depicted in Fig. 5.

Photobleaching, on the other hand, is a primary mechanism for limiting the solarization in BK-7. To substantiate this, we first solarized a site at high fluence and then lowered the fluence. Subsequent repeated exposure at a fixed lower fluence per pulse lowered the induced absorption coefficient to a new steady-state level. Importantly, the photobleaching was incomplete. We measured a 50% to 80% residual one-photon absorption after photobleaching to a new steady state. This very likely indicates that only certain induced absorption sites can absorb 532 nm radiation. Consequently, we infer that 2PA at 532 nm can induce more than one type of optical absorption site in BK-7.

As shown in the uppermost curve of Fig. 5, complete saturation of the solarization in BK-7 could not be obtained at the highest fluences used.

This was due to the delayed onset of catastrophic laser-induced damage, which would occur suddenly and unpredictably after repeated exposure at a fixed fluence per pulse through a fixed site. The damage tended to occur at a higher fluence for BK-7 (22-30 J/cm^2) than for BK-3 or BK-10 (10-17 J/cm^2). Further, the damage in BK-7 tended to occur at the back surface of the sample, but the damage in BK-3 and BK-10 tended to occur in the bulk glass.

The saturation of solarization in BK-7 has important practical consequences. It establishes a worst-case upper bound on the absorption which one can induce in long-term, high-intensity laser applications of BK-7. Figure 6 shows that the steady-state absorption in BK-7 is roughly proportional to fluence. From the slope of Fig. 6 we infer that the maximum induced solarization in BK-7 is about 0.004 cm^{-1} per J/cm^2 of fluence for our pump pulse. Normalizing this result by our temporal pulseshape factor $H^{(2)}$, which was measured to be 0.06×10^9 s^{-1}, we conclude that the maximum induced absorption in BK-7 at 532 nm is about 0.07 cm^{-1} per GW/cm^2 of pulse intensity.

Discussion

A simple kinetics model describes the preceding results. Solarization is attributable to color-center formation -- that is, to various charge-trapping mechanisms.[15,16] The net rate of color center formation, N_{cc}, is the rate at which charge trapping sites become occupied minus the rate at which color centers are annihilated, i.e.

$$\dot{N}_{cc} = \dot{N}^{+}_{cc} - \dot{N}^{-}_{cc} \quad . \tag{10}$$

Let us assume the fluence per shot and the laser repetition rate both are constant and that N_o, the total number of charge-trapping sites per unit volume of glass, is much greater than N_{cc}, the number of color centers. Then for a two-photon creation of color centers, the growth rate is proportional to the product of the number of unoccupied defect sites and the square of the intensity integrated over the pulse duration:

$$\dot{N}_{cc}^{+} = a\, H^{(2)} \Gamma^2 (N_o - N_{cc}) \simeq a\, H^{(2)} \Gamma^2 N_o \quad . \tag{11}$$

For a one-photon annihilation, the destruction rate is proportional to the product of the number of color centers and the fluence:

$$\dot{N}_{cc}^{-} = b\, \Gamma\, N_{cc} \quad . \tag{12}$$

Therefore in steady state the number of color centers, and hence the induced absorption, is proportional to fluence,

that is,

$$N_{cc} = \frac{a}{b} H^{(2)} \Gamma\, N_o \quad . \tag{13}$$

This agrees with the results displayed in Fig. 6.

From Smakula's equation [17], one can make a coarse estimate of the number of color centers per unit volume if one considers the induced absorption near 532 nm (Fig. 4) to be due to only one type of color center. Assuming a Gaussian lineshape function with a relative full width at half maximum of $2\Delta\omega/\omega = 0.34$ (inferred from Fig. 4), taking the effective mass of the color-center charge equal to the free-electron mass, and assuming an oscillator strength of unity and an absorption coefficient of 0.07 cm^{-1}, one obtains $N_{cc} = 0.8 \times 10^{15}\ cm^{-3}$. This corresponds to an absorption cross section of $8.8 \times 10^{-17}\ cm^2$.

Since the maximum induced absorption at 532 nm in BK-7 is 0.07 cm^{-1} per GW/cm^2, one has from Eq (13) that the color center density (per cm^3) is

$$N_{cc} = 0.8 \times 10^{15} H^{(2)}_{\Gamma}, \qquad (14)$$

where $H^{(2)}_{\Gamma}$ is in GW/cm^2

This rough estimate assumes that all of the induced absorption near 532 nm is due to a single inhomogeneously broadened transition. Clearly from Fig. 4 such an approximation is not rigorously justified. The small, wide spectral peak near 532 nm contributes only a fraction to the total absorption; most of the absorption is due to the tail of the ultraviolet peak (or peaks).

To account for multiple types of color center, one introduces more equations like Eqs. (9)-(11) plus any necessary cross-coupling terms.[15] The total optical absorption is then the sum of the absorptions due to each type of color center. To the extent that the coupled rate equations may be treated as linear differential equations with constant coefficients, the total absorption should rise as a sum of exponential terms toward a saturating value, with one term per species of color center. From Fig. 7, a graph of one of the curves from Fig. 5, one sees that the data do not fit a straight line on a semilogarithmic plot. Therefore, more than one type of color center is required to describe the laser-induced solarization in BK-7. This is consistent with our earlier observations and with previous ionizing radiation damage studies of boron-containing glasses.[16]

Considering its simplicity, our model explains the observed solarization in BK-7 quite satisfactorily. Nevertheless, it does not agree with all the observed facts. Chiefly, the initial slopes of the solarization growth curves (Fig. 5) vary roughly as the 4.5±1 power of fluence. This super-quadratic variation with fluence cannot easily be seen from Fig. 5, but it is clear when one examines the raw data. Furthermore, we have verified this in separate experiments with other BK-7 samples. Such behavior disagrees with the quadratic dependence expected from Eq. (11) and could indicate absorption by excited color-centers.[2] Additionally, important artifacts are expected in the thermal lensing signal, because the solarization is spatially non-uniform. The dependence of the induced absorption upon transverse pump beam intensity causes the total absorption coefficient ($\beta^{(m)}$ in Eq. (2)) to be expressible as a power series in fluence, Γ. This leads to higher-order fluence-dependent terms in the thermal lensing signal, S (Eq. (6)).

Summary

With a photothermal lensing technique we have measured two-photon absorption coefficients and have observed 2PA-induced solarization at 532 nm in the transparent borosilicate optical glasses BK-3, BK-7, and BK-10. BK-7, which has a smaller band gap energy than BK-3 or BK-10, shows a much stronger two-photon absorption and exhibits more solarization than the other two glasses. One-photon photobleaching quenches the 2PA-induced solarization. For a given temporal pulse shape and fluence per shot, the maximum induced absorption in BK-7 for long-term repeated exposure is 0.07 cm^{-1} per GW/cm^2.

The glasses we examined are chemically and structurally complex. Our measurements and simple solarization kinetics indicate that several types of color center contribute to the solarization. Further work is warranted in order to identify specific charge-trapping and photobleaching mechanisms.

It should be emphasized that the two-photon absorption coefficients in these glasses are extremely small (cm/TW), and the rates of solarization are sufficiently slow so that neither 2PA nor solarization in borosilicate glasses will be a problem in most laser applications at 532 nm. However, from a basic scientific view, two-photon absorption in glass has not been widely studied, and this work establishes a quantitative connection between two fundamental optical processes in certain transparent optical glasses.

Acknowledgments

The authors wish to express their thanks to Lee Cook (Schott Glass Technologies, Inc.) and Douglas Blackburn (National Bureau of Standards) for providing samples, to Tom Hindley (LLNL) for giving technical assistance, and to Allan Rosencwaig (Therma-Wave, Inc.) for helpful suggestions in the early phases of this work.

References

1. A. J. Twarowski and D. Kliger, "Multiphoton absorption spectra using thermal blooming," Chem. Phys. 20, North Holland Publishing Co., 253-264 (1977).
2. W. L. Smith, C. L. Vercimak, and W. E. Warren, "Excited-state-absorption cross-section in ultraviolet glasses following two photon absorption," J. Opt. Soc. Am. 72, 1782 (1982) and W. L. Smith, 1982 Laser Program Annual Report, Lawrence Livermore National Laboratory, UCRL-50021-82, p. 7.34-7.38.
3. W. F. Hagen and E. Snitzer, "Nonlinear Solarization in Flint Glasses by Intense 0.53μm Light," IEEE J. Quantum Electron. QE-4, 361 (1968).
4. W. L. Smith, 1981 Laser Proram Annual Report, Lawrence Livermore National Laboratory, UCRL-50021-81, p. 7.20-7.24; and P. Liu, W. L. Smith, H. Lotem, J. H. Bechtel, N. Bloembergen, and R. S. Adhav, Phys. Rev. B17, 4620 (1978).
5. M. A. Olmstead and N. M. Amer, "A new probe of the optical properties of surfaces," J. Vac. Sci. Technol. B1, 751-3 (1983).
6. W. B. Jackson, N. M. Amer, A. C. Boccara, and D. Fournier, "Photothermal deflection spectroscopy and detection," Appl. Opt. 20, 1333-44 (1981).
7. See, for example, Photoacoustic and Photothermal Spectroscopy, J. Badoz and D. Fournier, Eds., J. Phys. (Paris) 44 Colloq. (C6), (October 1983).
8. M. Bass, E. W. Van Stryland and A. F. Stewart, "Laser calorimetric measurement of two-photon absorption," Appl. Phys. Lett. 34 (2), 142-4 (1979).

9. E. A. McLean, L. Sica, and A. J. Glass, "Interferometric observation of absorption induced index change associated with thermal blooming," Appl. Phys. Lett. 13 (11), 369-71 (1968).

10. M. A. Henesian, A. Rosencwaig, and M. J. Weber, 1981 Laser Program Annual Report, Lawrence Livermore National Laboratory, UCRL-50021-81, p. 7.31-7.33.

11 M. E. Long, R. L. Swofford, and A. C. Albrecht, "Thermal lens technique: a new method of absorption spectroscopy," Science 19, 183-4 (1976).

12. W. T. White, III, unpublished.

13. See, for example, S. E. Stokowski, R. A. Saroyan, and M. J. Weber, "Nd-Doped Laser Glass Spectroscopic and Physical Properties," Lawrence Livermore National Laboratory, Report M-95, Rev. 2 (1981).

14. M. J. Weber, D. Milam, W. L. Smith, "Nonlinear Retractive Index of Glasses and Crystals," Opt. Engr. 17, 463-469 (1978).

15. P. W. Levy, P. L. Mattern, K. Lengweiler, and A. M. Bishay, "Studies on nonmetals during irradiation: V, growth and decay of color centers in barium aluminoborate glasses containing cerium," J. Am. Ceramic Soc. 57 (4), 176-181 (1974).

16. R. Yokota, "Color centers in alkali silicate and borate glasses," Phys. Rev. 95, 1145-48 (1954).

17. W. B. Fowler, Physics of Color Centers, Academic Press, N.Y. (1968), Eq. (2-45).

Table 1. Temperature derivative of optical path length and specific heat of BK-3, BK-7, and BK-10 at constant external pressure and 300 K.

Glass	$(\frac{\partial n}{\partial T})_p$ [a]	$(\frac{\partial \ell}{\partial T}/\ell)_p$ [a]	C_p	$n(633\ nm)$ [a]	$\frac{\partial(n\ell-\ell)}{\partial T}/\ell$
	$(10^{-6}K^{-1})$	$(10^{-6}K^{-1})$	$(J/cm^3/K)$		$(10^{-6}K^{-1})$
BK-3	3.5	5.3	1.82 [b]	1.497	6.1
BK-7	1.5	7.1	2.15 [a]	1.515	5.2
BK-10	2.1	5.8	1.77 [b]	1.496	5.0

(a) Schott Glass Technologies, Inc., Optical Glass Catalogue.

(b) T. Hoheisel, Lawrence Livermore National Laboratory, Private Communication.

Table 2. Measured two-photon absorption coefficients at 532 nm (2ω = 4.67 eV) and approximate band edge energies (eV) for BK-3, BK-7, and BK-10.

Glass:	BK-3	BK-7	BK-10
β(cm/TW)	0.6 ± 0.6	2.9 ± 1.5	0.4 ± 0.4
Band edge (eV)*	4.4	4.0	4.5

*Defined as the photon energy at which the absorption coefficient equals 1.0 cm^{-1}.

Figure Captions

1. Layout for two-beam photothermal lensing experiments. (H, half-wave plate; P, Glan polarizer, A1, A2 and A3, apertures; L1, L2 and L3, lenses; BS1, BS2 and BS3, beam splitters; W_o, plane of probe beam waist; F1 and F2, optical filters; S', equivalent sample plane for beam diagnostics.)
2. Temporal profile of second harmonic pump beam from Nd:YAG laser. Average of 32 consecutive pulses.
3. Spatial profile of second harmonic pump beam obtained from video image analysis system. Average of 32 consecutive pulses.
4. Induced linear absorbance in solarized BK-7 glass as a function of wavelength. The unsolarized BK-7 spectrum has been subtracted out. (See text for conditions of irradiation.)
5. Solarization-induced linear absorption $\alpha(N)$ in BK-7 as a function of number of laser pulses N at axial fluences of 12, 16, and 26 J/cm^2.
6. Steady-state values of solarization-induced absorption $\alpha(\infty)$ as a function of axial fluence.
7. Approximation of solarization growth as a multi-exponential process.

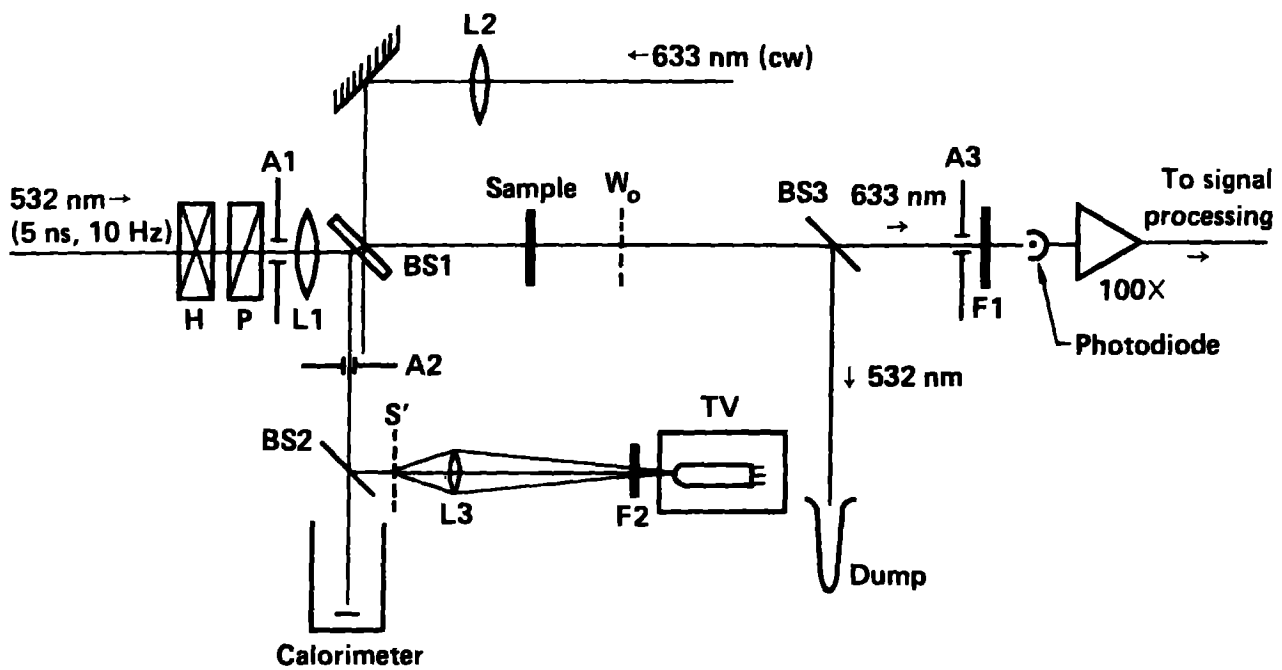
L2
←633 nm (cw)
A1
532 nm→
(5 ns, 10 Hz)
Sample
W_o
BS3
633 nm
→
A3
To signal
processing
→
100X
H
P
L1
BS1
F1
Photodiode
A2
↓ 532 nm
S'
TV
BS2
L3
F2
Dump
Calorimeter

Figure 1

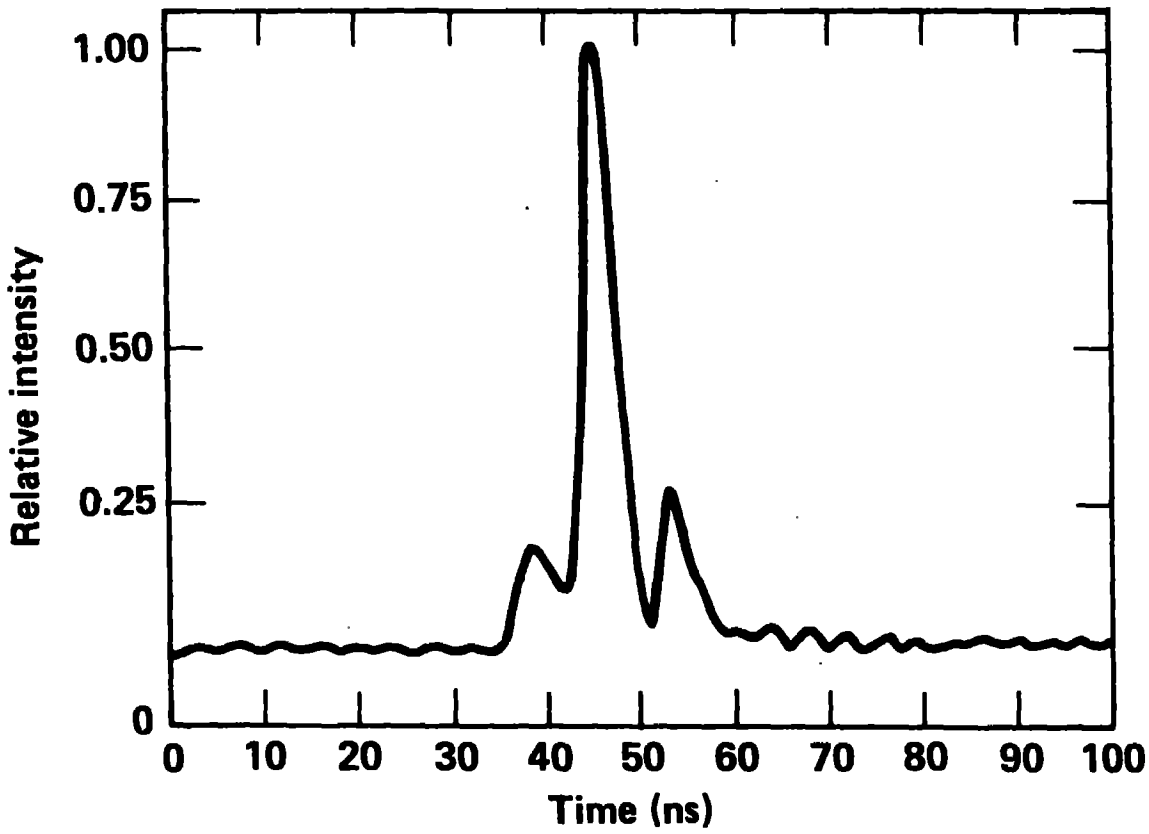
1.00
0.75
0.50
0.25
0
Relative intensity
0
10
20
30
40
50
60
70
80
90
100
Time (ns)

Figure 2

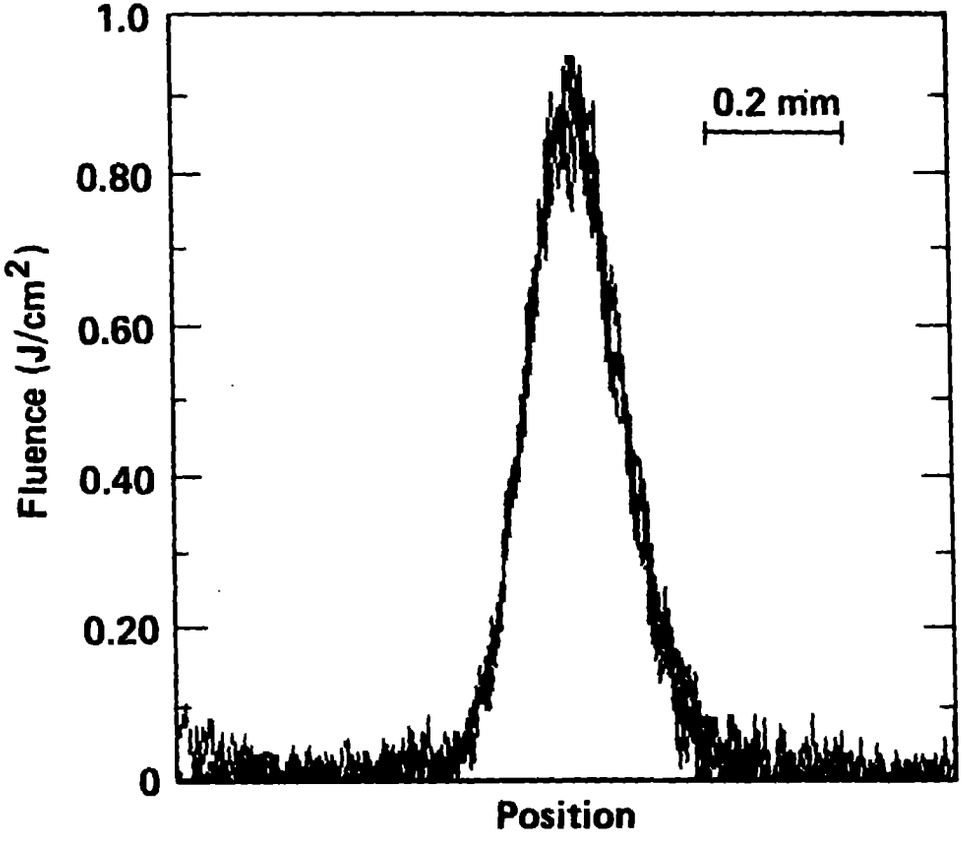

Figure 3

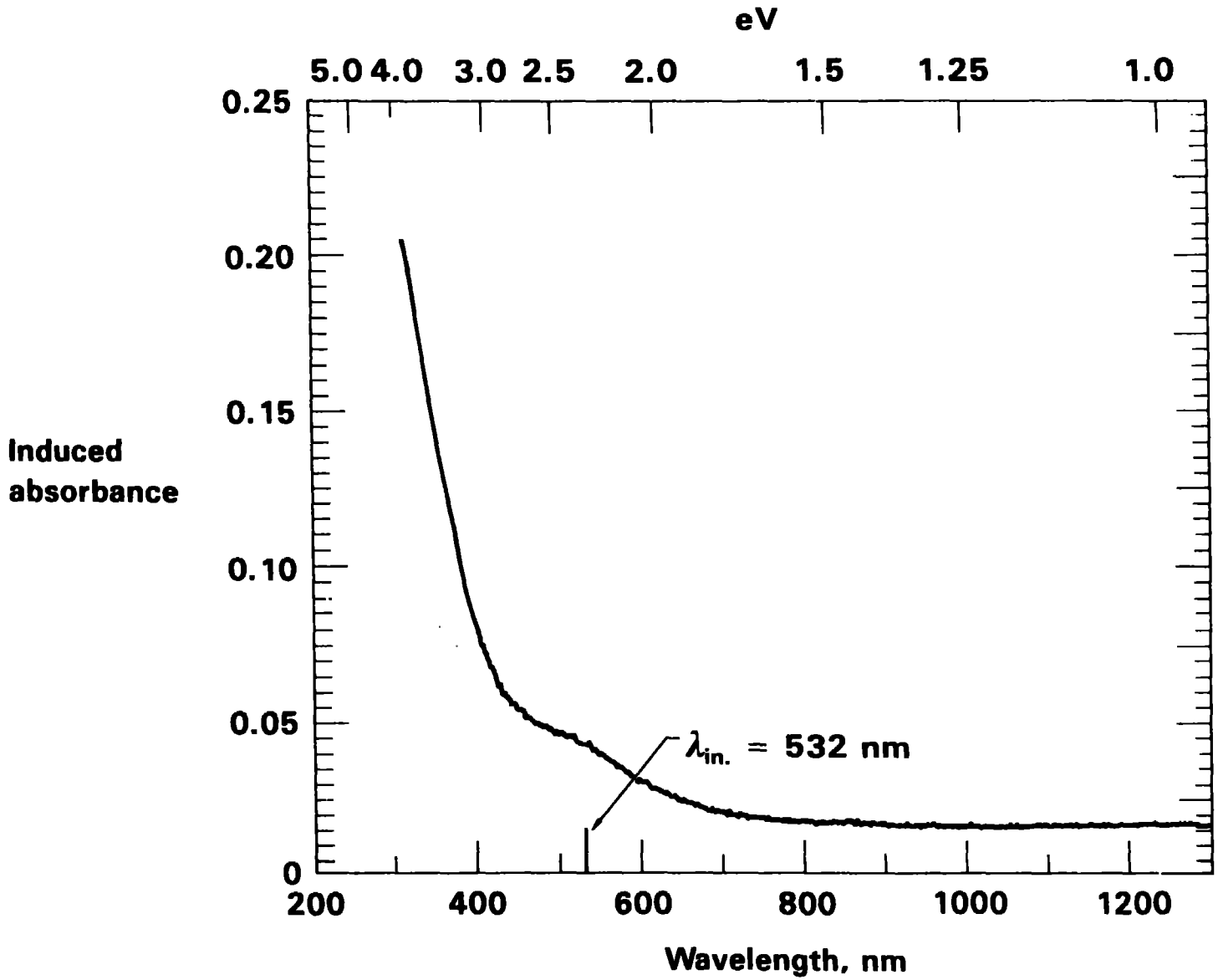
eV
5.0 4.0 3.0 2.5 2.0 1.5 1.25 1.0
0.25
0.20
0.15
0.10
0.05
0
Induced absorbance
$\lambda_{in.}$ = 532 nm
200 400 600 800 1000 1200
Wavelength, nm

Figure 4

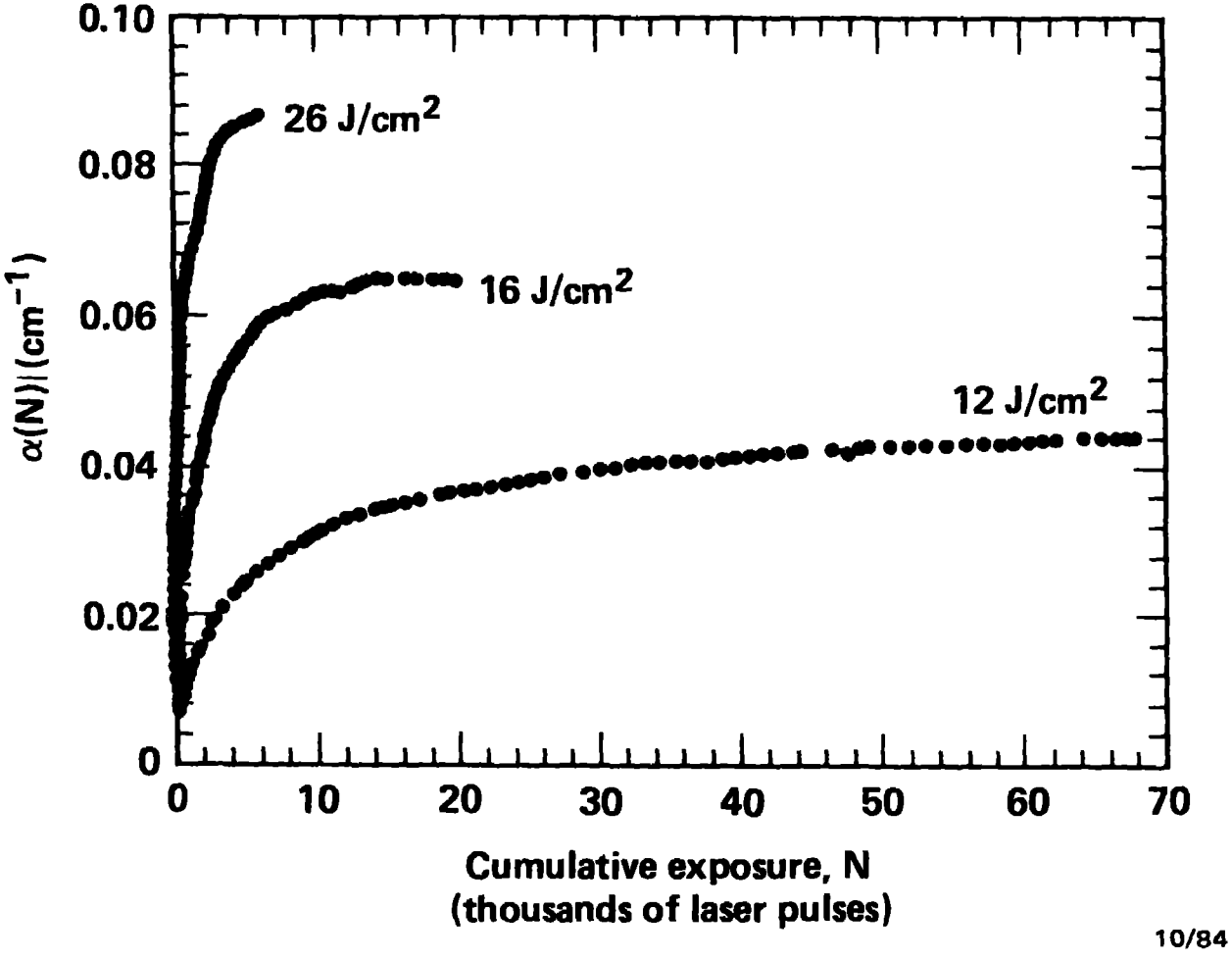
0.10
0.08
0.06
0.04
0.02
0
α(N)|(cm⁻¹)
26 J/cm²
16 J/cm²
12 J/cm²
0
10
20
30
40
50
60
70
Cumulative exposure, N
(thousands of laser pulses)
10/84

Figure 5

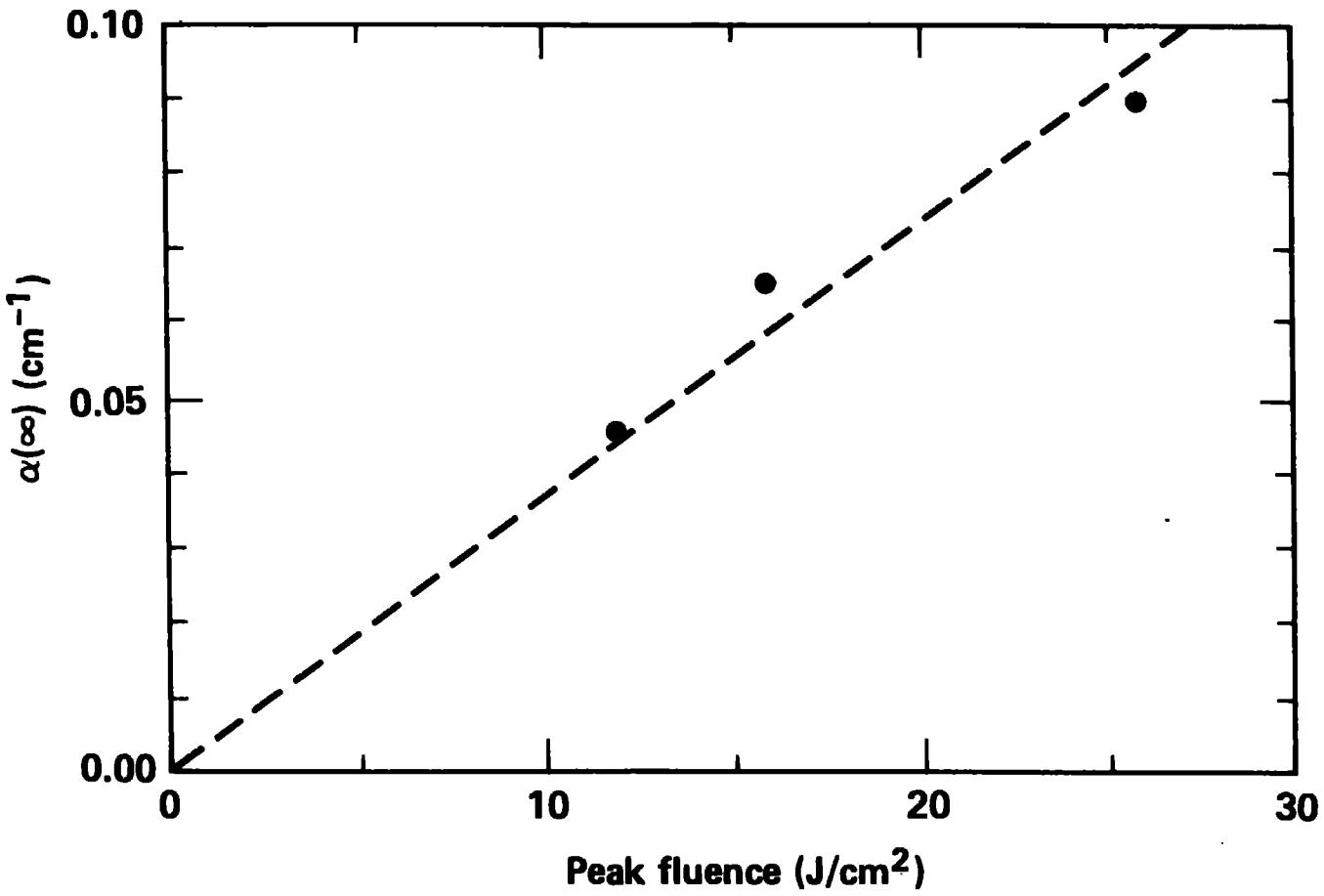

Figure 6

10/84

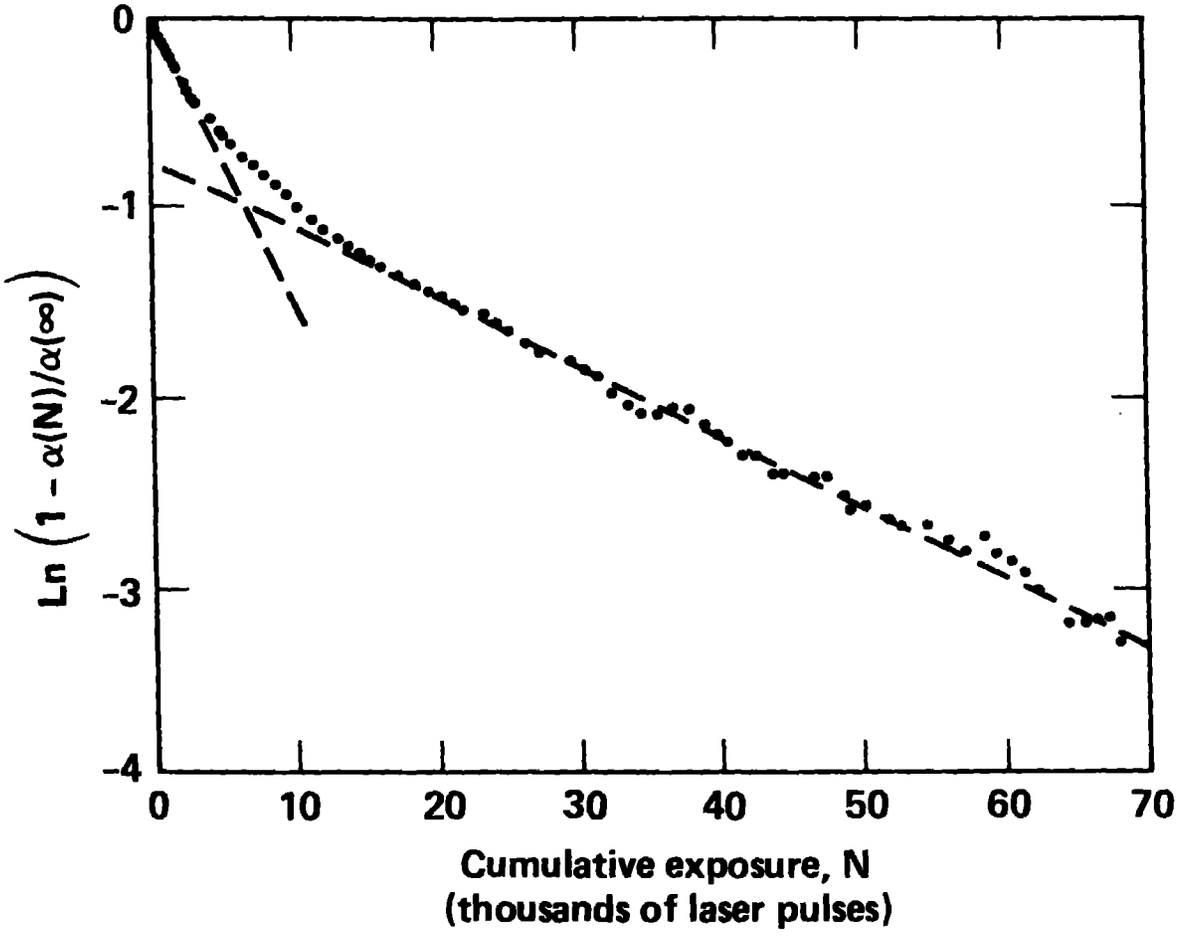

10/84

Figure 7